Lab Notes

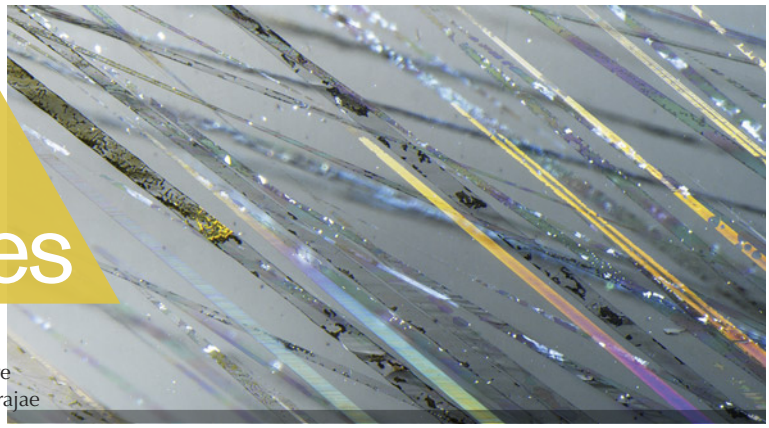

Editors

Thomas M. Moses | Shane F. McClure
Sally Eaton-Magaña | Artitaya Homkrajae

Green HAÜYNE

The Carlsbad laboratory recently examined a suite of seven yellowish green to bluish green gems ranging in weight from 0.24 to 1.44 ct (figure 1), which were identified as haüyne, a member of the sodalite group. Gem-quality haüyne is most notable for its intense blue color, especially in material of German origin, so the striking green color of these stones was unexpected. However, a deposit of green haüyne was reported from Afghanistan earlier this year (B. Srisataporn et al., "Green haüyne: A rarity among sodalite gems," *Journal of Gemmology*, Vol. 39, No. 1, 2024, pp. 13–16).

Standard gemological testing revealed properties consistent with haüyne, including an average refractive index of 1.50 and a hydrostatic specific gravity of 2.41. The stones also fluoresced orange to long-wave UV and were inert to short-wave UV. Microscopic examination revealed interesting whitish inclusions, which have been previously reported as mica (figure 2). This was confirmed by Raman spectroscopy. No evidence of clarity enhancement was observed in any of the stones examined. Raman spectroscopy further confirmed the identity of the green gems as haüyne.

This suite represents the first green gem-quality haüyne examined by GIA and is an interesting and rare collector stone.

Nathan Renfro, Maxwell Hain, and Wim Vertriest

Figure 1. These seven stones (0.24–1.44 ct) ranging in color from yellowish green to bluish green were identified as the rare gem haüyne.

Figure 2. A large mica cluster was observed in the 1.44 ct green haüyne; field of view 1.83 mm. Courtesy of Bill Vance.

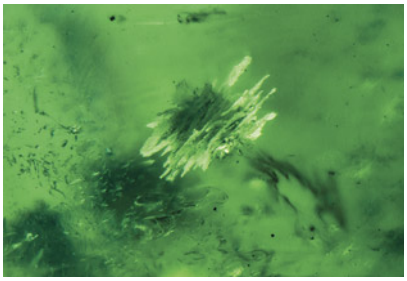

LABORATORY-GROWN DIAMOND

Colored Bands in CVD-Grown Diamond

The Surat laboratory recently examined a 3.14 ct F-color oval brilliant diamond grown by chemical vapor deposition (CVD). The diamond featured a single dark brown band measuring ~2.2 mm in length that resembled graining in natural diamond (figure 3). The band was visible under the microscope as well as with a 10× loupe. The clarity grade was VVS_2 based on this colored band, which was visible through multiple bezels and affected the transparency at that location. Through the pavilion, parallel whitish bands were also observed (figure 4A).

Editors' note: All items were written by staff members of GIA laboratories.

Gems & Gemology, Vol. 60, No. 3, pp. 368–380.

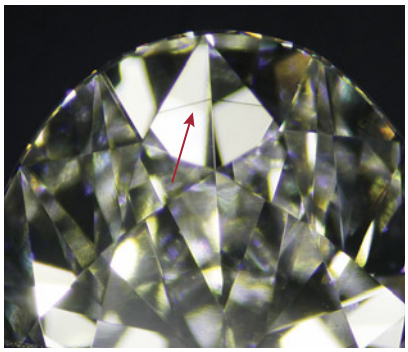

Figure 3. A growth remnant appeared as a color band (arrow) in a 3.14 ct CVD-grown diamond. Field of view ~11.75 mm.

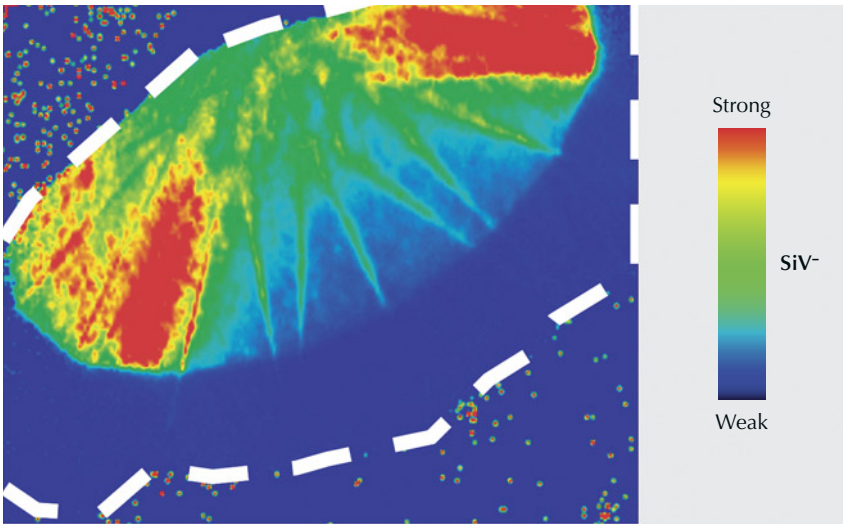

Figure 5. False-color PL map of the SiV^- defect at 736.6/736.9 nm using 633 nm laser excitation, normalized to the diamond Raman area on the pavilion. The dashed line indicates the approximate outline of the diamond.

The subtle banding seen in this diamond differed from a cloud of graphite inclusions at a growth interface previously reported in a CVD-grown diamond (Summer 2023 Lab Notes, pp. 213–214). The fluorescence image collected by the DiamondView revealed a layered growth structure that did not coincide with the color banding, indicating a start-stop cycling growth process typical of CVD synthesis (figure 4B). Deep UV fluorescence with green and blue coloration as well as strong green phosphorescence seen in the DiamondView image (figure 4C) indicated high-pressure, high-temperature treatment. The SiV^- defect at 736.6 and 736.9 nm, a common feature of CVD laboratory-grown diamond and only rarely seen in natural diamond, was observed in photoluminescence (PL) spectra using 457, 514, and 633 nm laser excitation. PL mapping (figure 5) revealed that the concentration of SiV^- was higher near the culet of the pavilion and dramatically lower near the table.

GIA has documented growth remnants in thousands of CVD-grown diamonds. But with a multitude of manufacturers, recipes, and treatments, a wide variety of clarity characteristics are encountered, including the unusual color band observed here.

Srushti Tanti and Raju Jain

Irradiated HPHT-Grown Diamonds with Blue-Green Color Zonation

The Carlsbad laboratory received two diamonds grown by the high-pressure, high-temperature (HPHT) process that contained interesting color

Figure 4. A: Hazy parallel lines (indicated by arrows) resembling whitish internal graining; field of view ~6.31 mm. DiamondView imaging of the pavilion facets showed blue growth layers in green fluorescence (B), as well as strong green phosphorescence (C).

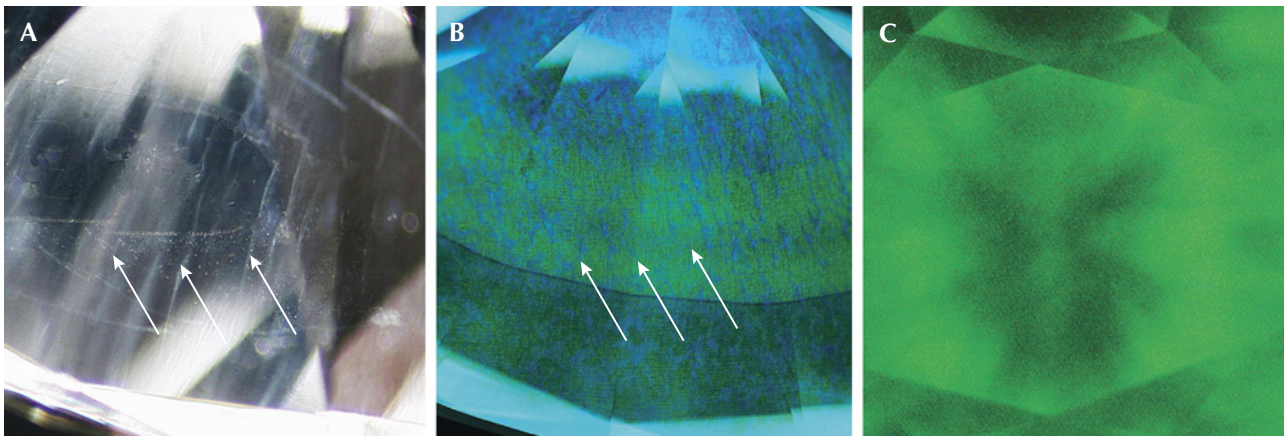

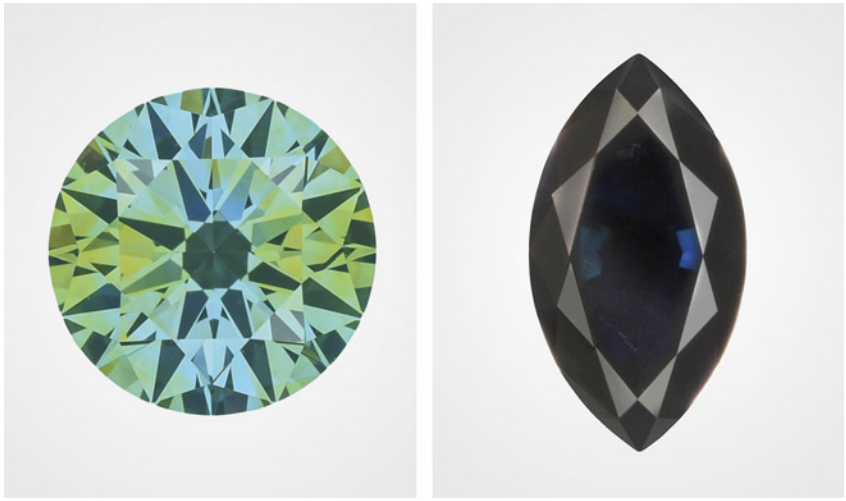

Figure 6. Two HPHT-grown diamonds: a 0.51 ct round brilliant with Fancy Deep bluish green color (left) and a 1.56 ct Fancy black marquise (right).

zonation. The 0.51 ct round brilliant (figure 6, left), submitted for a laboratory-grown colored diamond report, received a Fancy Deep bluish green color grade. The 1.56 ct marquise (figure 6, right), submitted for the same LG-CD service, was Fancy black. Both stones were determined to be artificially irradiated. The high concentration of defects created by laboratory irradiation led to extensive absorption in the marquise, causing a black appearance that is fairly uncommon for laboratory-grown diamonds. When viewed through the pavilion, sector-dependent color zonation was visible in both stones (figure 7).

Dramatic color zonation corresponding with growth sectors is a feature of some fancy-color HPHT-grown diamonds (J.E. Shigley et al., "Gemesis laboratory-created diamonds," Winter 2002 *G&G*, pp. 301–309; J.E. Shigley et al., "Lab-grown colored diamonds from Chatham Created Gems," Summer 2004 *G&G*, pp. 128–145; S. Eaton-Magaña et al., "Observations on HPHT-grown synthetic diamonds: A review," Fall 2017 *G&G*, pp. 262–284; Winter 2023 Lab Notes, pp. 489–490). In these particular irradiated stones, the areas of transmitted blue color were due to the GR1 defect, which created absorption primarily in the red portion of the visible spectrum (e.g., C.D. Clark et al., "The absorption spectra of natural and irradiated diamonds," *Proceedings of the Royal Society of London A: Mathematical, Physical, and Engineering Sciences*, Vol. 234, No. 1198, 1956, pp. 363–381). Nitrogen can cause absorption in the blue portion of the visible spectrum to contribute to yellow color in some of the growth sectors, and together these can lead to a combined green color. From the pavilion of the round brilliant diamond (figure 7, left), the yellow sectors appeared to be distinct from blue, but these color components combined to appear green face-up (figure 6, left). Similarly, green coloration resulting from yellow Ib and blue IIb sectors was described in some early HPHT-grown diamonds (Shigley et al., 2004).

These stones offer examples of fun and distinctive features that can be observed in laboratory-grown colored diamonds.

Taryn Linzmeyer and Sally Eaton-Magaña

PEARLS

Fashioned Queen Conch Shell Bead

Conch pearls are prized for their porcelaneous surface and distinctive flame-like pattern, characterized by a regular arrangement of parallel elongated crystals that create a silky sheen (H.A. Hänni, "Explaining the flame structure in non-nacreous pearls,"

Figure 7. Viewed through the pavilion, sector-dependent color zones were apparent in both the round brilliant (left) and the marquise (right; field of view 7.19 mm).

SSEF, 2009). Highly valued Queen conch pearls, produced by the *Aliger gigas* species (formerly *Strombus gigas* or *Lobatus gigas*), are known for their exquisite pink coloration, flame structure, and porcelaneous luster. Queen conch shells are widely used for crafting and jewelry accessories and sometimes used to simulate the appearance of natural pearls.

Recently, GIA's Mumbai laboratory received a drilled light pink bead for pearl identification, measuring 10.20 mm in diameter and weighing 7.50 ct (figure 8). Most Queen conch pearls are oval, semi-baroque, or baroque, and it is very rare to find a perfectly round conch pearl similar to the submitted specimen. In addition, an obvious banded structure was observed on the surface, which raised suspicions of a fashioned shell (E. Fritsch and E.B. Misiorowski, "The history and gemology of Queen conch 'pearls'," Winter 1987 *G&G*, pp. 208–221). The banded structure was arranged in a distinct concentric ring pattern resembling a bull's-eye (figure 9A), with alternating white, cream, and light pink bands covering half of its surface. The parallel band lines appeared to run throughout the bead when observed using transmitted fiber-optic illumination (figure 9B), consistent with the parallel striations revealed by real-time X-ray microradiography imaging (figure 9C). Under high magnification, prominent flame structures with long, slender linear striations were visible (figure 9D).

Figure 8. This round light pink bead fashioned Queen conch shell (10.20 mm and 7.50 ct) resembled a Queen conch pearl.

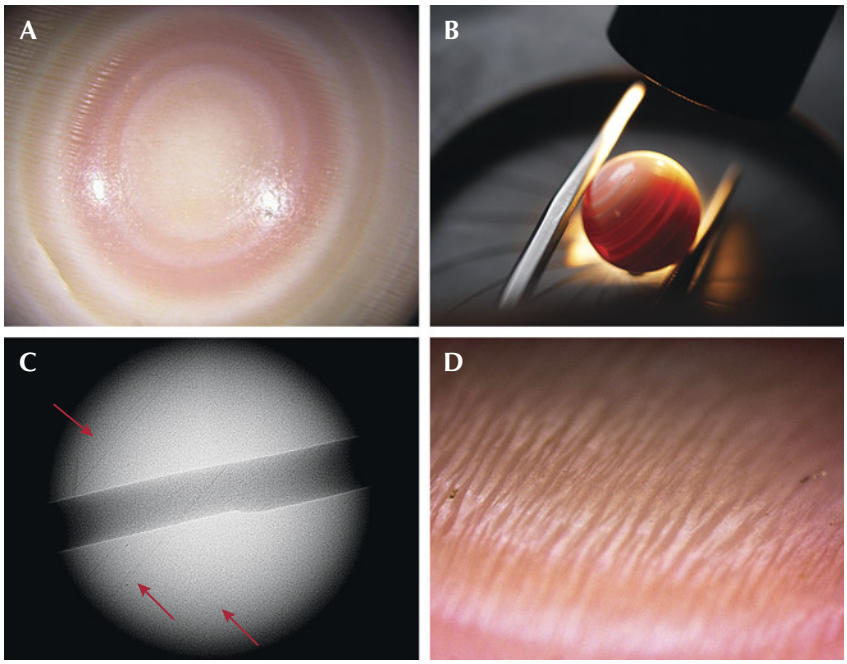

Figure 9. A: Concentric rings with alternating white, cream, and light pink color bands resembling a bull's-eye; field of view 3 mm. B: Banded structure observed under fiber-optic illumination. C: Internal banding lines (red arrows) correlating to the external bands visible in image A. D: A pattern of parallel elongated slender flames imparting a silky sheen effect; field of view 1 mm.

Ultraviolet/visible/near-infrared reflectance spectra showed absorption features at 280 and 368 nm and a broad band centered at 512 nm, similar to those seen in natural orangy pink conch pearls, confirming their natural color origin (figure 10). Raman analysis using 514 nm laser excitation revealed a doublet at 702/704 cm^{-1} and a peak at 1086 cm^{-1}, indicative of aragonite. Significant polyenic pigment peaks were previously observed at 1125 and 1514 cm^{-1}, indicative of natural color (S. Karampelas et al., "Raman spectroscopy of natural and cultured pearls and pearl producing mollusc shells," *Journal of Raman Spectroscopy*, Vol. 59, No. 1, 2019, pp. 1813–1821). After thorough analysis, the specimen was confidently determined to be a fashioned shell bead imitation originating from the shell of an *Aliger gigas* gastropod (Queen conch).

Shell imitations of pearl hold a long-standing history as fashionable jewelry pieces targeting a wide consumer base. These imitations are occasionally misrepresented as "shell pearls" or simply "pearls," potentially misleading less experienced buyers (Summer 2014 Lab Notes, pp. 153–154). Their close resemblance to natural and cultured pearls often leads consumers to seek laboratory testing. The fashioned shell specimen under examination was relatively straightforward given the distinctive banded structure, a feature normally absent in pearls. However, it is crucial to observe subtle traits and compositions that can distinguish genuine pearls from imitations. Shell is the most popular material used for porcelaneous pearl imitations, and sometimes it is sourced from the same mollusk

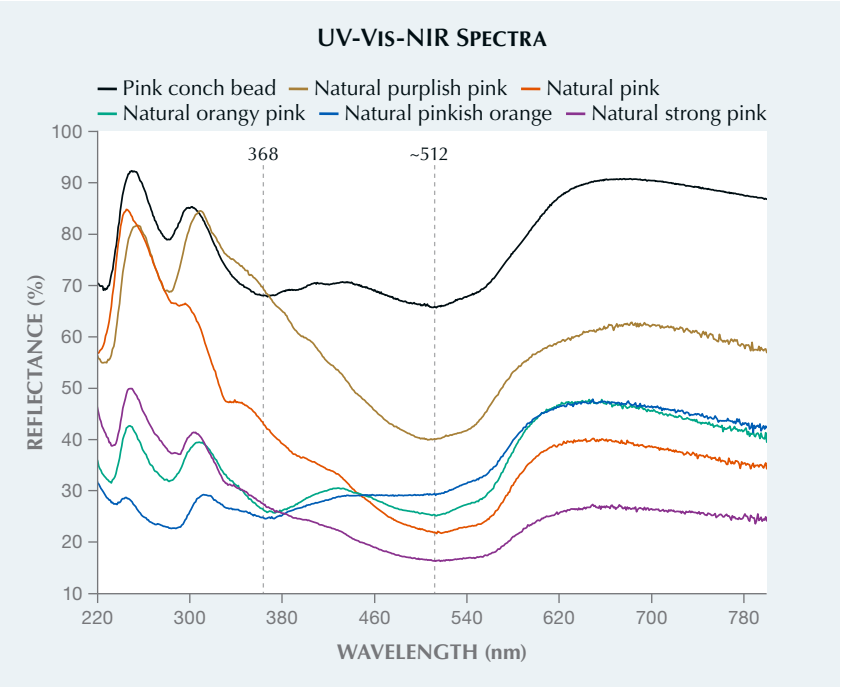

Figure 10. UV-Vis-NIR spectra comparison of the conch bead imitation with five naturally colored conch pearls from GIA reference samples. The natural orangy pink and pinkish orange samples displayed a feature at 368 nm with a broad reflectance band centered around 512 nm similar to that observed in the examined specimen.

species as the pearl being imitated, causing similar color and surface appearance. Therefore, caution and scrutiny are always essential when purchasing pearl products.

Gauri Sarvankar, Abeer Al-Alawi, and Roxane Bhot Jain

Two Imitation Melo Pearls

Flame structures are a surface characteristic of Melo pearls produced from mollusks belonging to the *Melo* species. The flame pattern is a result of the interaction of light with an interwoven aragonite lamellae microstructure of the pearl (H.A. Hänni, "Explaining the flame structure of non-nacreous pearls," *Australian Gemmologist*, Vol. 24, No. 4, 2010, pp. 85–88). Melo pearls are valued for their rarity, large sizes, attractive yellowish orange to orange colors, and flame structures. Therefore, it is not surprising that there have been attempts to imitate these pearls (M.S. Krzemnicki, "A worked shell bead as an imitation of a melo pearl," *Gemmological Journal Hong Kong*, Vol. 27, 2006, pp. 31–33; Summer 2006 Lab Notes, pp. 166–167; N. Sturman et al., "An imitation 'Melo pearl,'" *GIA Research News*, January 21, 2011). Most imitations of Melo pearl are dyed fashioned shells from the *Tridacna* species. However, two recent samples submitted to GIA for pearl identification were unusual.

The Hong Kong laboratory received a 140.58 ct orange sphere measuring 27.23 mm. At first glance, its orange bodycolor and non-nacreous surface appearance with a blotchy pattern resembled the flame-like surface structure of a Melo pearl (figure 11, left). However, high magnification revealed a mosaic structure and concentrations of an orange dye substance (figure 12). While aragonite and polyenic pigments are commonly observed in naturally colored Melo pearls, Raman spectroscopy indicated a calcite composition with diagnostic peaks at 282, 713, and 1088 cm^{-1}. Photoluminescence spectroscopy showed clear peaks at 552 and 560 nm, proving the presence of color treatment. This combined evidence confirmed the specimen was dyed calcite.

Meanwhile, another orange sphere (figure 11, right) weighing 89.81 ct and measuring 23.27 × 23.00 mm that appeared to be a Melo pearl was submitted to the Bangkok laboratory. The sample's color and appearance were similar to that of the specimen tested in Hong Kong, but its surface texture was mottled. Magnification revealed a patchy structure of unnat-

Figure 11. A 140.58 ct dyed calcite sphere (left) and an 89.81 ct round dyed and coated shell (right), both resembling Melo pearls.

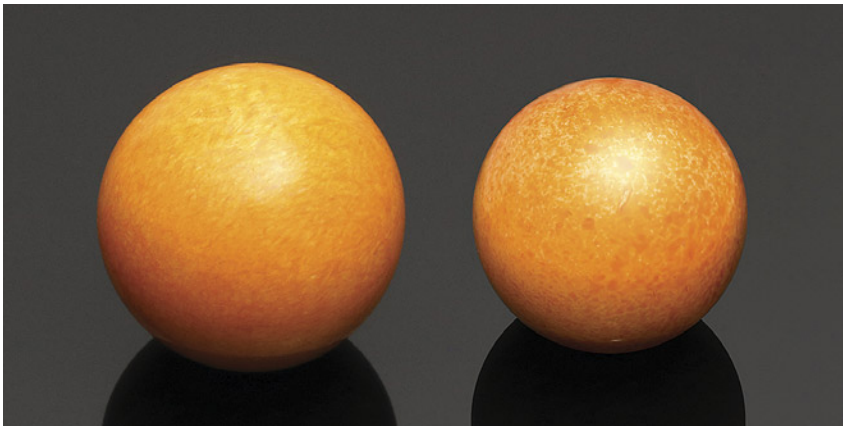

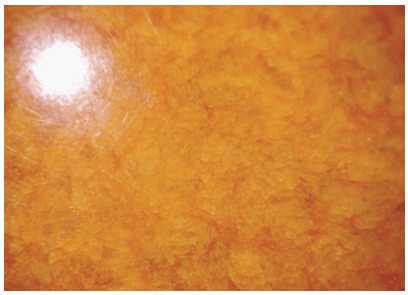

Figure 12. The 140.58 ct sphere exhibited a mosaic structure, and orange color concentration was noted within areas under magnification. Field of view 6.92 mm.

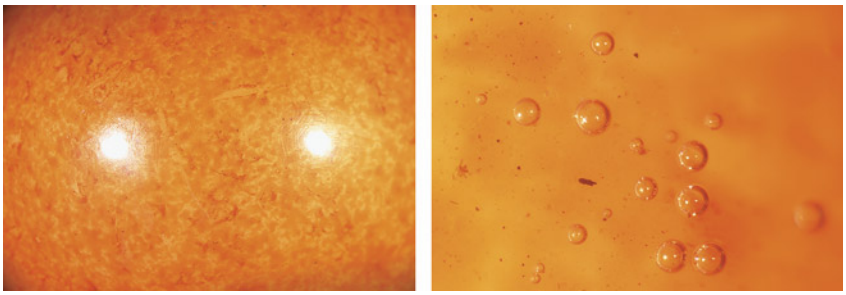

Figure 13. Microscopic observation of the 89.81 ct sphere revealed unnatural color patches (left) and gas bubbles and trapped dirt (right). Fields of view 19.20 and 1.80 mm.

ural orange coloration and a lack of flame patterns (figure 13, left). The sample possessed a resinous luster, and gas bubbles and trapped dirt suggested a colorless coating on the outermost surface (figure 13, right). The Raman spectroscopy of the coated surface showed distinct peaks around 1582, 1602, 2945, 3004, and 3065 cm^{-1}, indicative of an artificial resin (L. Kiefert et al., "Identification of filler substances in emeralds by infrared and Raman spectroscopy," *Journal of Gemmology*, Vol. 26, No. 8, 1999, pp. 501–520; Fall 2005 Gem News International, pp. 272–273). Under strong fiber-optic illumination, the item exhibited obvious banding typical of shell-related materials (figure 14, left). Furthermore, one area seemed to have been ground down, revealing a white material underneath the coated and dyed layers (figure 14, right). Raman analysis on the area showed peaks at 703, 1085, and 1460 cm^{-1}, identifying the material as aragonite. All the data obtained led to the conclusion that this was a Melo pearl imitation made of a dyed and coated shell.

While pearl imitations are not new to the market, these two samples appear strikingly similar to natural Melo pearls. Careful inspection under high magnification and advanced analytical procedures employed by gemological laboratories are sometimes needed to provide accurate and comprehensive results.

Wing Kiu Fan and Ravenya Atchalak

Metallic Core in a Natural Freshwater Pearl

Although cultured pearls dominate the freshwater pearl industry, the rarer natural freshwater pearls are still encountered during routine laboratory testing. The majority of these have been handed down through generations, and recent finds are limited due to heavy regulations in the mussel shelling industry and lower demand for mother-of-pearl. Recently, GIA's Mumbai laboratory received for identification a white circled button-shaped nacreous pearl measuring 5.74 × 3.98 mm and weighing 0.97 ct (figure 15).

The pearl displayed circular bands on its upper portion with minor sub-surface-reaching cracks and a translucent nacreous layer with

Figure 14. Left: A "banding test," performed using strong transmitted lighting to reveal banding, indicated the item was fashioned from shell. Right: The underlying white surface was exposed in one polished area; field of view 3.60 mm.

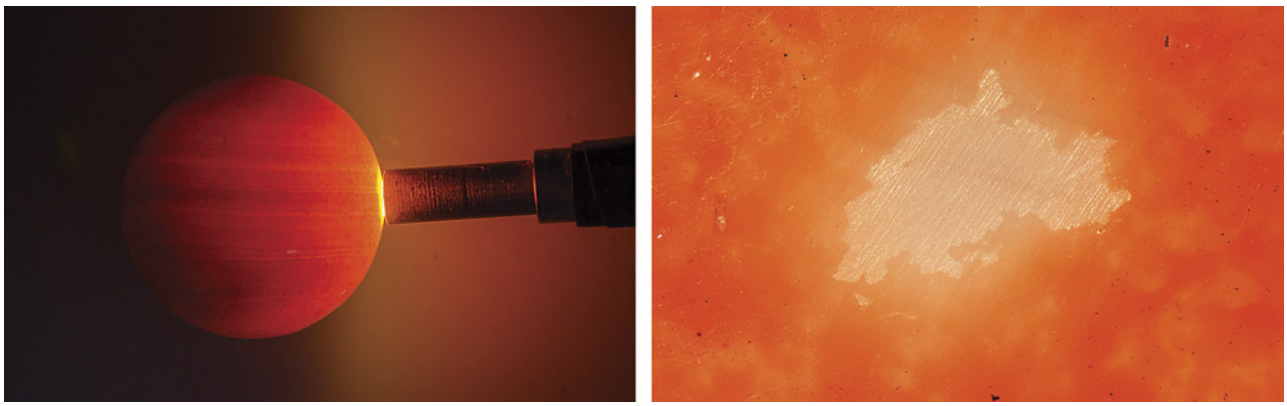

Figure 15. The white natural freshwater pearl measuring 5.74 × 3.98 mm and weighing 0.97 ct.

overlapping platelets of aragonite. The pearl showed a strong yellowish green reaction when exposed to X-ray fluorescence. Energy-dispersive X-ray fluorescence analysis conducted on two spots revealed manganese levels of 348 and 390 ppm and strontium levels of 470 and 694 ppm, respectively. The results of both analyses are characteristic of pearls from a freshwater environment. Under long-wave ultraviolet light, the pearl exhibited a moderate greenish yellow reaction, which is typical for unprocessed white pearls. White cultured freshwater pearls are routinely processed and show moderate to strong blue reactions under long-wave UV.

Real-time X-ray microradiography (RTX) imaging revealed a small near-round radiopaque white core, measuring approximately 0.20 × 0.15 × 0.12 mm, surrounded by concentric growth arcs extending to the pearl's edge (figure 16). The core's radiopacity suggested it was composed of a material of higher density than the surrounding nacreous area. This resembled the opacity typically observed in metals during X-ray radiography and was similar to metal cores previously noted in saltwater pearls (M.S. Krzemnicki, "Pearl with a strange metal core," *SSEF Facette*, No. 24, 2018, p. 27; Summer 2023 Gem News International, pp. 244–246). Another metal remnant was observed in the pearl's drill hole, initially presumed to be a fragment of a broken needle used during drilling (figure 16).

Upon closer examination using X-ray computed microtomography (µ-CT), the metal feature within the drill-hole area appeared similar to the metallic core found within the pearl and seemed to be partially embedded within the pearl's growth arcs. Both metal features exhibited undulating outlines and a lack of sharp edges typically associated with a broken metal fragment. Given the similar properties of both metal fea-

Figure 16. Left: RTX imaging from the side reveals a near-round metallic core (yellow arrow) surrounded by growth arcs and a small metal feature within the drill hole (red arrow). Right: RTX imaging from the top reveals slight distortion to the metal core and a small metal feature embedded inside the wall of the drill hole.

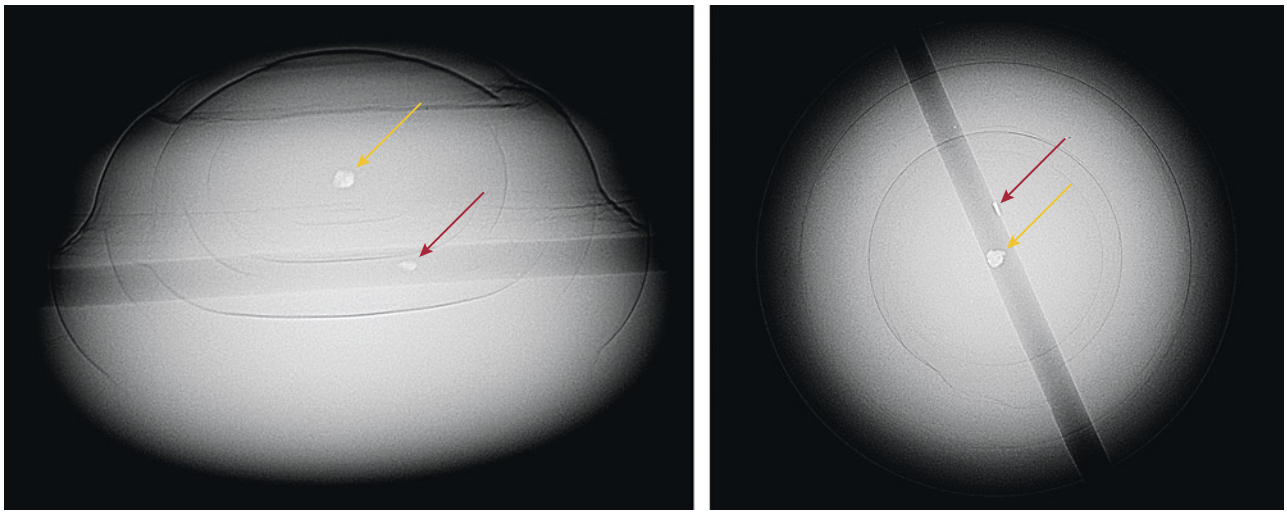

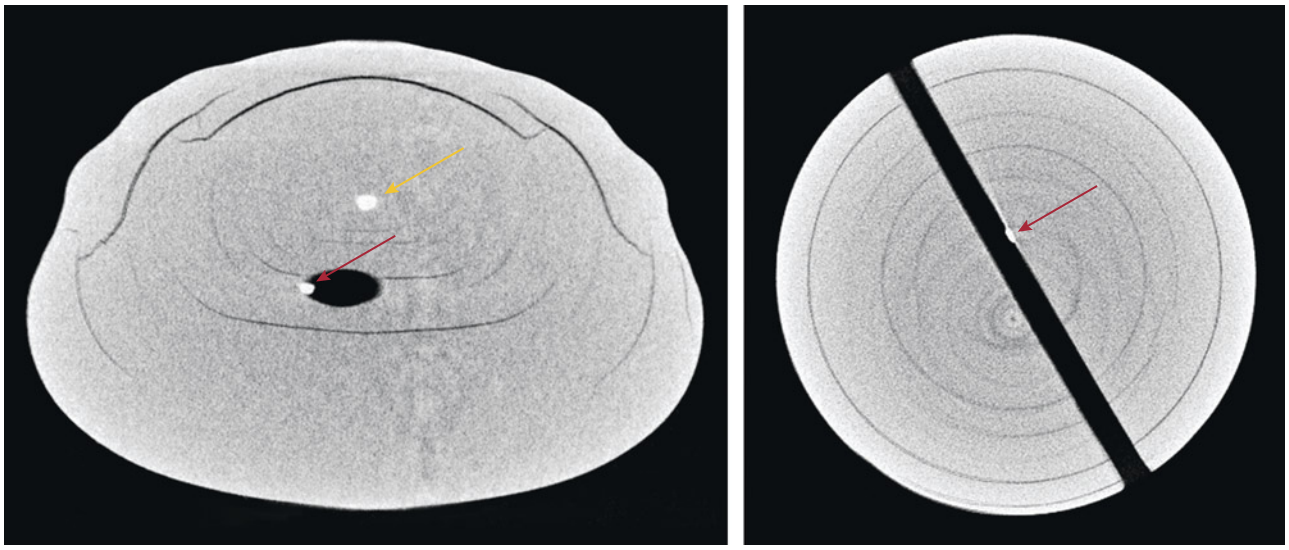

Figure 17. Left: µ-CT image showing the metallic core (yellow arrow) and the small metal feature crossing the boundary of the drill hole (red arrow). Right: µ-CT image showing only the metal feature protruding from a nacreous area in the drill hole (red arrow).

tures, the metal feature at the drill hole may have been present prior to the drilling process, rather than a remnant from a drilling needle (figure 17).

Because RTX and µ-CT imaging did not reveal any suspicious irregular linear or void structures typically found at the center of freshwater cultured pearls, the sample was identified as a natural freshwater pearl (K. Scarratt et al., "Characteristics of nuclei in Chinese freshwater cultured pearls," Summer 2000 *G&G*, pp. 98–109). The structure present was comparable to that of natural freshwater pearls previously studied by GIA (Summer 2021 Gem News International, pp. 167–171). The only difference noted was the metallic core at the center of this pearl, a feature not commonly observed in natural freshwater pearls.

These observations suggest environmental contamination during the pearl's formation, potentially due to the presence of a foreign object around which the pearl formed. The process of pearls forming around such foreign objects remains a topic of ongoing scientific research.

Jayesh Surve and Abeer Al-Alawi

A Multicore Non-Bead Cultured Pearl

Recently, the Mumbai laboratory received a lot consisting of 101 variously shaped, white to cream saltwater nacreous loose pearls for identification services. When exposed to X-ray fluorescence (XRF), the pearls showed an inert to weak yellowish green reaction. Energy-dispersive X-ray fluorescence confirmed the saltwater origin of these pearls; however, an unusually high concentration of strontium was detected on the surface, which will be the subject of a separate study.

Real-time X-ray microradiography (RTX) imaging showed typical non-bead cultured pearl structures, mostly with central dense cores surrounded by concentric growth rings and associated light gray calcium carbonate ($CaCO_3$) "seed" features, elongated linear structures, and sizeable spindle-shaped voids (A. Homkrajae et al., "Internal structures of known *Pinctada maxima* pearls: Cultured pearls from operated marine mollusks," Fall 2021 *G&G*, pp. 186–205). Some of the pearls contained multiple nuclei that showed varied combinations of multicore structures. One of these was a light cream near-oval pearl weighing 1.69 ct and measuring 6.83 × 5.34 mm that exhibited a bumpy cluster-like formation (figure 18). Under long-wave ultraviolet radiation, the pearl displayed a moderate yellowish green reaction typical of white pearls from the *Pinctada* species.

Figure 18. A semi-baroque non-bead cultured pearl weighing 1.69 ct and measuring 6.83 × 5.34 mm.

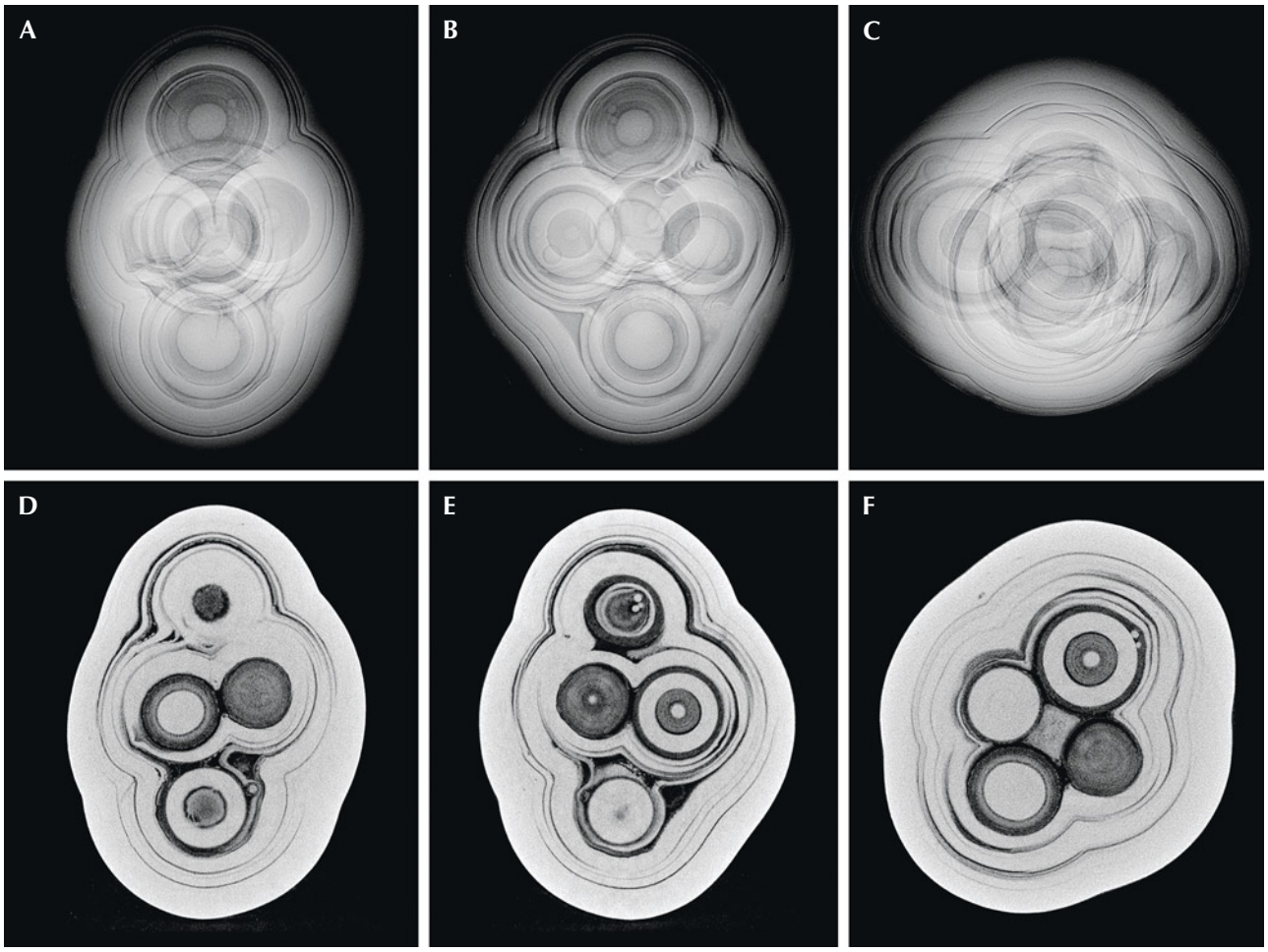

Figure 19. Top: RTX images revealing the pearl's complex multicore internal structure. Bottom: µ-CT images displaying the six cores present inside the pearl.

The pearl showed an inert reaction when subjected to XRF, consistent with others in the group and characteristic of a saltwater environment. Raman spectroscopy using 514 nm laser excitation detected a doublet at 701 and 704 cm^{-1}, along with a main peak at 1086 cm^{-1}, indicating the presence of aragonite.

RTX imaging in three directions revealed a complex interconnected structure within the pearl, and several cores of varying sizes and radiopacities overlapped, making it difficult to count the number of cores (figure 19, A–C). X-ray computed microtomography (µ-CT) analysis displayed the structure more clearly, showing a total of six medium to large light gray dense cores engulfed by distinct conchiolin-rich layers (figure 19, D–F). Four cores exhibited prominent light gray calcium carbonate "seed" features in the organic-rich concentric growth rings. Such features are commonly observed in non-bead cultured pearls from the *Pinctada maxima* species (Homkrajae et al., 2021). Notably, two of the cores were encircled by thick alternating concentric growth rings with radiopacities of lighter and darker shades of gray. All the cores were surrounded by growth layers conforming to the pearl's shape, and the "seed" features were also observed in between the layers, as shown in the video at www.gia.edu/gems-gemology/fall-2024-lab-notes-multicore-nonbead-cultured-pearl.

Considering its external appearance, internal structure, and saltwater environment, the pearl was classified as a non-bead cultured pearl from the *Pinctada maxima* species.

Both natural and cultured pearls commonly exhibit multiple nuclei structures. Most natural pearls with multiple nuclei contain internal growth arc structures, and multicores of significant size inside the organic-rich concentric structures are generally related to non-bead cultured pearls. However, it is rare to encounter pearls with more than a couple of cores, making this pearl unique and noteworthy. Ongoing research is currently being conducted to further study the unusual chemistry readings recorded in the lot of pearls received.

Roxane Bhot Jain, Karan Rajguru, Abeer Al-Alawi, and Chunhui Zhou

Figure 20. This necklace contains 63 variously colored and shaped Mexican pearls from Pteria *and* Pinctada *species and the Pinnidae family, measuring from 4.88 mm to 10.75 × 9.32 mm.*

Natural Pearl Necklace from Baja California Sur, Mexico

A unique necklace containing 63 pearls of various colors, shapes, sizes and mollusk species (*Pteria* and *Pinctada* species, and Pinnidae family) was recently submitted to the Carlsbad laboratory for examination (figure 20). Ranging in size from 4.88 mm to 10.75 × 9.32 mm, all the pearls were nacreous and exhibited overlapping aragonite platelets under high magnification, and the majority displayed a pronounced orient or iridescence phenomenon.

Interestingly, several pearls displayed similar crosslines with various surface patterns, seen in figure 20. The crosslines appeared to be natural grooves with no signs of surface treatment. Further testing identified these as *Pteria* pearls.

Nine pearls of light yellowish brown to brown colors displayed a similar linear-looking nacre appearance caused by slender rectangular aragonite platelets, which has been observed on the nacreous surface of *Pinna* or pen pearls belonging to the Pinnidae family (figure 21; E. Strack, *Pearls*, Rühle-Diebener-Verlag, Stuttgart, Germany, 2006; N. Sturman et al., "Observations on pearls reportedly from the Pinnidae family (pen pearls)," Fall 2014 *G&G*, pp. 202–215). The nacre of pearls from the *Pteria* and *Pinctada* species generally consists of hexagonal or polygonal aragonite platelets.

Under long-wave ultraviolet radiation, many of the pearls exhibited weak to strong orangy red to red fluorescence, which is characteristic of the porphyrin pigment found in colored *Pteria* pearls (figure 22; L. Kiefert et al., "Cultured pearls from the Gulf of California, Mexico," Spring 2004 *G&G*, pp. 26–38). The fluorescence intensity of the *Pteria* pearls varied depending on their darkness and color saturation.

Figure 21. A linear-looking nacre is characteristic of nacreous Pinna *or pen pearls from the Pinnidae family; field of view 3.68 mm.*

Figure 22. The Pteria*,* Pinctada*, and* Pinna *pearls displayed distinct fluorescence colors under long-wave ultraviolet radiation: orangy red to red (*Pteria*), green to greenish yellow (*Pinctada*), and chalky yellow (*Pinna*).*

The samples with more intense colors displayed a stronger red reaction. In contrast, darker pearls from the *Pinctada* species exhibited weaker green to greenish yellow reactions. The pen pearls showed a weak to moderate chalky yellow fluorescence, consistent with the reaction of some pen pearls (Sturman et al., 2014).

Real-time X-ray microradiography (RTX) revealed various growth patterns of natural pearls. Many *Pteria* samples contained a typical large dark gray organic-rich area in the center, and a faint radial structure was also present within the dark area in some samples (figure 23). One pen sample exhibited an irregular dark gray void associated with light gray granular features that was previously observed in some natural nacreous pen pearls (Sturman et al., 2014) and in GIA's research collection.

Energy-dispersive X-ray fluorescence (EDXRF), ultraviolet/visible reflectance spectroscopy, and photoluminescence spectroscopy using a 514 nm laser excitation analyses indicated that all the pearls were of saltwater origin and naturally colored.

The client who submitted the necklace noted that the pearls were reportedly fished from the coastlines of the Mexican state of Baja California Sur, from both the Pacific Ocean and the Gulf of California (Sea of Cortez), over the course of eight years. The *Pteria* pearls were fished near San Carlos and Guerrero Negro, the pen pearls from the San Ignacio lagoon and Muleje, and the *Pinctada* pearls from Loreto. Based on the geographical information provided and the gemological characteristics observed, the mollusk species can be more precisely determined. The *Pteria* and *Pinctada* pearls likely came from *Pteria sterna* and *Pinctada mazatlanica*, respectively, as both species are indigenous along Mexico's Pacific coast and the Gulf of California (M. Cariño and M. Monteforte, "History of pearling in La Paz Bay, South Baja California," Summer 1995 *G&G*, pp. 88–105; Strack, 2006). Although the Pinnidae family is widespread globally, pen pearls from *Atrina tuberculosa* (often called *Atrina maura*) are local to Mexico and noted to produce pearls with a partially nacreous surface (Strack, 2006).

Mexico has been a rich source of pearls since ancient times (Cariño and Monteforte, 1995). Overfishing, changes in water environment, and dam construction have shortened the lifespan of indigenous mollusks and limited pearl production since the end of the nineteenth century (D. McLaurin-Moreno, "Sea of Cortez pearls: A historical overview," *Sixteenth Annual Sinkankas Symposium—Pearl*, Gemological Society of

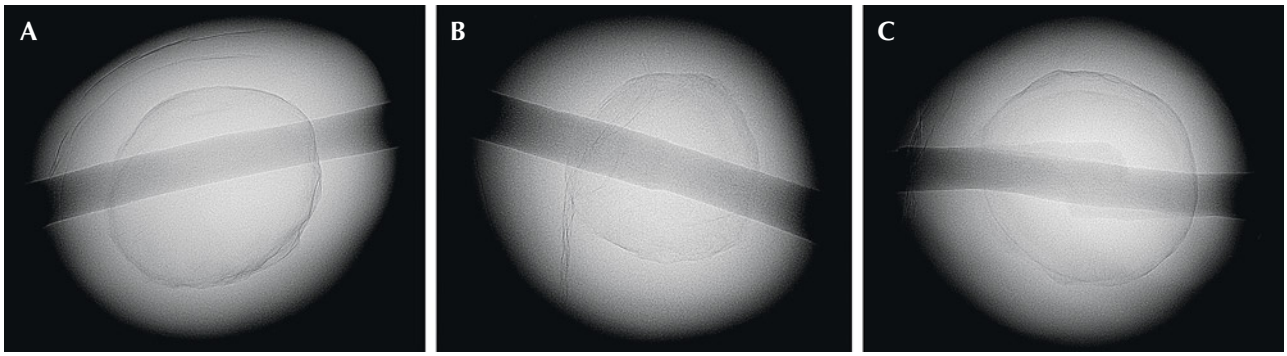

Figure 23. A large dark gray organic-rich area is a typical structure in natural Pteria *pearls, and sometimes a faint radial structure is found within the dark area.*

San Diego and GIA, pp. 6–29). These new pearls from native species signal the return of healthy mollusk beds.

Artitaya Homkrajae and Amiroh Steen

Iridescent Tubes in PEZZOTTAITE

A large 8.13 ct emerald-cut purplish pink pezzottaite ($CsLiBe_2Al_2Si_6O_{18}$) was submitted to the Carlsbad laboratory for gem identification (figure 24). Pezzottaite is a member of the beryl mineral group. This specimen had a measured refractive index of 1.600–1.610 and a specific gravity of 3.06. This stone was exceptional for its large size and quality, and gemological testing revealed no evidence of clarity treatment. The identity of the specimen was verified using Raman and Fourier-transform infrared spectroscopy, which also revealed the presence of H_2O in the crystal structure channels of the specimen, a common feature in pezzottaite. While the clarity of this pezzottaite was impressive for this mineral, especially without enhancement, the overall transparency was diminished by the presence of inclusions and small fractures. Some of these inclusions, such as the growth bands and tubules, could be considered distinctly beautiful features. Although the stone itself had a purplish pink hue, in darkfield illumination it appeared dark pink-purple (figure 25). The sample exhibited faint growth banding, with thin tube inclusions approximately perpendicular to the growth banding (i.e., tubes imperfectly parallel to the *c*-axis, crossing at shallow angles, and banding nearly perpendicular to the *c*-axis). At some viewing angles, the tube inclusions displayed vivid iridescence ranging from magenta, purple, neon blue, and green, to neon yellow and orange, given appropriate illumination. The iridescence was more vivid in darkfield

Figure 24. This 8.13 ct pezzottaite contains delicate growth banding (~horizontal) and tube inclusions (~vertical, seen best in lower left).

Figure 25. Iridescent tube inclusions (bottom left corner in figure 24) in pezzottaite, shown in darkfield illumination; field of view 2.5 mm.

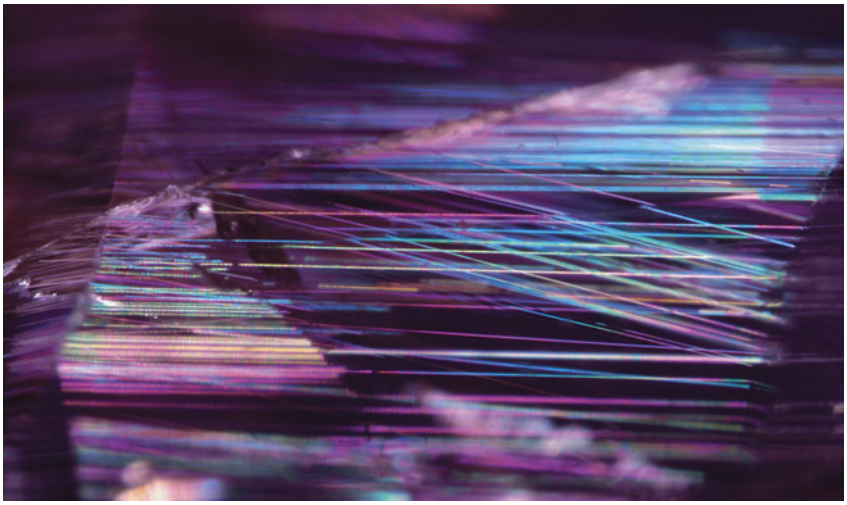

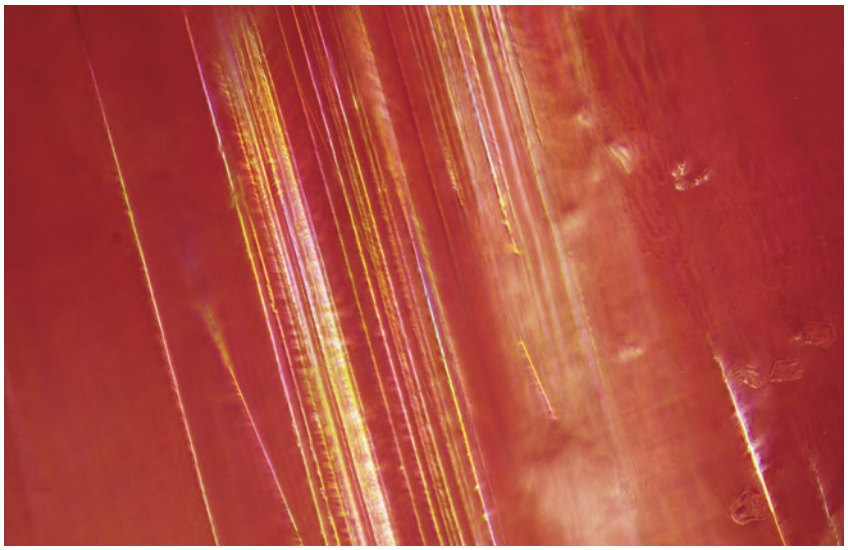

Figure 26. Iridescent growth tubes in pezzottaite with brightfield illumination; field of view 0.72 mm.

illumination, but brightfield lighting showed a pinkish orange background which made the tubes shimmer (figure 26). Although colorful in specialized microscope lighting, the tubular inclusions were semitransparent white to the unaided eye in common lighting conditions.

Rhiana Elizabeth Henry, Taryn Linzmeyer, and Jeffrey Hernandez

RUBY with Synthetic Overgrowth Lining Cavities

GIA's Bangkok laboratory recently received an 8.63 ct purplish red marquise double cabochon. The stone showed gemological properties consistent with ruby: a spot refractive index of 1.770 and a characteristic ruby spectrum using a handheld spectroscope. It was semitransparent and contained altered growth tubes, multiple fractures with flux residues, and some fractures with trapped flattened gas bubbles and areas of filled cavities. X-ray fluorescence revealed significant amounts of lead, mostly along fractures and filled cavities.

The author observed an unusual area of granular texture lining the filled cavity (areas of lower luster) (figure 27). This granular texture was caused by a reaction layer of synthetic overgrowth where surfaces were melted and recrystallized. This pattern can be found in any high-temperature heat-treated corundum. Synthetic overgrowth at the surface of a stone can sometimes be removed by repolishing.

Sudarat Saeseaw

PHOTO CREDITS
Annie Haynes—1, 20; Nathan Renfro—2; Raju Jain—3, 4A; Suraj Maurya—4 (B and C); Rhonda Wilson—6; Taryn Linzmeyer—7 (right), 26; Gaurav Bera—8, 9, 15, 18; Johnny (Chak Wan) Leung—11 (left); Lhapsin Nillapat—11 (right); Cheryl (Ying Wai) Au—12; Ravenya Atchalak—13, 14 (right); Nuttapol Kitdee—14 (left); Artitaya Homkrajae—21, 22; Adriana Robinson—24; Rhiana Elizabeth Henry—25; Polthep Sakpanich—27

Figure 27. An area of a filled cavity in ruby exhibiting a lower luster than the ruby and surrounded by a granular texture, caused by a reaction layer of synthetic overgrowth. Reflected light (left) and brightfield illumination (right); field of view 8.2 mm.